Rainwater-driven transport of matter and microbes from phyllosphere to soil in a temperate beech forest

Authors

Markus Krüger[1], Karin Potthast[2,3], Beate Michalzik[2,3], Alexander Tischer[2,3,4], Martina Herrmann[1,3,5*]

Affiliations

[1]Institute of Biodiversity, Ecology and Evolution, Friedrich Schiller University Jena, Jena, Germany; [2]Department of Soil Science, Friedrich Schiller University Jena, Jena, Germany; [3]German Center for Integrative Biodiversity Research (iDiv) Halle-Jena-Leipzig, Leipzig, Germany, [4]ThüringenForst, Forestry Research and Competence Centre, 99867 Gotha, Germany, [5]Cluster of Excellence Balance of the Microverse, Friedrich Schiller University Jena, Jena, Germany,

*Corresponding author:

Martina Herrmann

martina.herrmann@uni-jena.de

ORCID

Markus Krüger: 0000-0003-1709-6806

Karin Potthast: 0000-0001-5657-065X

Beate Michalzik: 0000-0001-7858-1771

Alexander Tischer: 0000-0003-2923-8330

Kirsten Küsel: 0000-0002-5396-0975

Martina Herrmann: 0000-0001-8330-8585

Abstract

In forest ecosystems, the transport of organic matter including microbial cells by throughfall and stemflow represents a central linkage between the phyllosphere and soil. However, the extent and taxon-specificity of rainwater-mediated vertical transfer of microorganisms, and its relevance for matter fluxes is sparsely understood. We investigated the rainwater-driven transport of bacteria and its contribution to matter transport in bulk rainfall, throughfall, stemflow and seepage in a temperate deciduous forest and compared the transported communities to those in phyllosphere and soil. Throughfall-mediated cell fluxes equaled those in seepage below the litter layer, pointing to a substantial above-ground translocation of bacteria. Bacterial cells contributed up to 11 % and 33 % to the exported total organic carbon and total nitrogen, respectively. Bacteria affiliated with *Pseudomonadaceae*, *Oxalobacteraceae*, *Hymenobacteraceae*, and *Sphingomonadaceae* were differentially transmitted from the canopy with increased abundances in throughfall and stemflow compared to bulk rain. A small fraction of shared taxa pointed to the import, proliferation and mobilization of selected bacterial taxa between neighboring ecohydrological compartments. The genetic potential of the transported bacterial communities was strongly linked to organic matter degradation particularly of carbohydrates and proteins. Our findings extend our understanding of rainwater-mediated vertical matter transport in forest ecosystems and highlight the contribution of microbial cells to this transport especially in above-ground compartments. Strong shifts in community composition and abundance of the transported taxa between throughfall, stemflow and soil seepage are linked to differences in source communities but may also point to different mechanisms of cell detachment across compartments.

Keywords

throughfall, stemflow, seepage, microbial transport, carbon fluxes, nitrogen fluxes

Highlights

- Rainwater flow paths are important carriers for organic matter and microorganisms.
- Throughfall and stemflow contained high abundances of microbial cells.
- Bacteria contributed up to 11 % and 33 % to exported carbon and nitrogen.
- Bacterial taxa were selectively mobilized by throughfall, stemflow and seepage.

1. Introduction

Rainwater represents an important carrier of various particles including organic matter and microorganisms across long distances (Hu et al., 2018). Such wet deposition may harbor tens of millions of bacteria m^{-2} d^{-1} (Reche et al., 2018) and other microorganisms such as archaea, fungi and protists (Després et al., 2012; Sánchez-Parra et al., 2021), and thus plays a crucial role in microbial dispersal within ecosystems. Microbes from atmospheric sources may contribute directly to the microbiome of the plant phyllosphere (Ponette-González et al., 2020), which exhibits a global surface area of 6.4 x 10^8 km^2 as microbial habitat (Vorholt, 2012). During rain events, huge amounts of rainwater can pass the forest canopy and emerge as throughfall and stemflow water fluxes (Levia et al., 2011). Throughfall represents that part of precipitation which falls through the canopy, partially along leaf surfaces, while stemflow is defined as the flow path of rainwater which runs down the stem (Sadeghi et al., 2020). In temperate forests, both water flow paths can transport a substantial amount of organic matter ranging between 0.2 – 200 kg C ha^{-1} y^{-1} (Ponette-González et al., 2020; Van Stan et al., 2017) and bacteria in the range of 1.5 x 10^{16} cells ha^{-1} yr^{-1} (Bittar et al., 2018). As consequence, the forest canopy may act as a considerable source of microorganisms, influencing the bacterial composition of rainwater as it is transported down to the forest floor (Sadeghi et al., 2020; Van Stan et al., 2017). A certain proportion of this rainwater further percolates through the soil as seepage, containing mobile organic matter including microorganisms (Dibbern et al., 2014; Herrmann et al., 2023; Krüger et al., 2021), overall resulting in above-ground and below-ground microbial transport patterns .

In the phyllosphere, bacteria perform a variety of matter transformation processes such as carbon- and nitrogen fixation, nitrification and methanol oxidation (Andrews and Harris, 2000; Guerrieri et al., 2020). Methanotrophic bacteria such as *Methylomonas* and *Methylobacter, Flavobacterium* and *Novosphingobium* are common members of the microbiome on tree leaf and bark surfaces (Jeffrey et al., 2021; Vorholt, 2012). In addition, microbial extracellular enzymes which degrade hydrocarbons and secondary plant metabolites can be exported from

the phyllosphere by throughfall and stemflow (Mori et al., 2019), contributing to exoenzymatic matter degradation in the soil. In contrast to litter fall in autumn, which acts as a periodic mass transfer of organic matter, microorganisms, and their degradation capacity to the forest floor, throughfall and stemflow represent season-independent, high-frequency episodic flow events from the phyllosphere, ensuring connectivity between above-ground and below-ground compartments and associated matter transfer throughout the year.

Assuming a certain fraction of the microbial cells remains viable during transport, rainwater delivers air- and phyllosphere-derived bacteria which constitute an essential source of new genetic material and functional potential to the sink communities. In fact, previous work demonstrated that some bacteria are selectively washed off from leaves and stems and get enriched along the water flow paths (Guerrieri et al., 2020; Teachey et al., 2018). Stemflow creates funneling of water along with matter and microbes which are rapidly transported along roots into the soil (Carlyle-Moses et al., 2020). In addition, rainwater provides fresh particulate and biolabile dissolved carbon and nitrogen to the forest floor (Michalzik et al., 2001; Van Stan and Stubbins, 2018), which can affect soil nutrient pools (Van Stan et al., 2017) and soil microbial activity (Deng et al., 2017).

Previous studies investigated the microbial diversity and mass fluxes associated with aerosol particles (Després et al., 2012), tree phyllosphere, throughfall and stemflow (Van Stan et al., 2020). However, research is scarce on the quantity and structure of microbial communities transported by rainwater, throughfall, and stemflow, on which fraction of the transported matter originates from microbial cells, and on how their functional potential differs across different compartments including soil seepage. Seepage-mediated transport of microbes through soils was previously studied at the Hainich Critical Zone Exploratory using lysimeters installed in a beech forest (Krüger et al., 2021; Herrmann et al., 2023). In this study, we used zero tension lysimeters along with bulk rainwater, throughfall and stemflow collectors (Levia et al., 2023; Potthast et al., 2017) to investigate the abundance and community composition of bacteria along neighboring ecohydrological compartments ranging from the tree canopy to the soil.

These compartments included rainwater, phyllosphere, throughfall, stemflow, seepage and soil. In addition, we predicted the functional potential of these communities and their contributions to matter fluxes. We aimed to (1) estimate bacterial fluxes and contributions to carbon and nitrogen transport in throughfall, stemflow and seepage, comparing an early and late growing season rain event; (2) characterize the bacterial composition of the respective compartments and their predicted functional potential, and (3) assess core and shared communities for each intersection of neighboring compartments to provide insights into the fraction of bacterial communities that is subject to throughfall-, stemflow- or seepage-mediated mobilization.

2. Materials and methods

2.1 Study site and sampling procedure

Sampling was conducted in spring and autumn on a managed deciduous temperate forest plot (N51°06'56.5' E10°24'45.2) and on an open area site (N51°07'63.5' E10°23'68.2') in the Hainich-Dün area comprising the Hainich Critical Zone Exploratory, Germany (**Figure 1A**). Forest stands are dominated by European beech (*Fagus sylvatica* L.) with minor admixtures of sycamore maple (*Acer pseudoplatanus* L.) and ash (*Fraxinus excelsior* L.), a common forest composition in the Hainich-Dün area. A nearby, extensively managed grassland site (open area) was used for measurements of bulk precipitation (rainwater). The climate is characterized by annual precipitation of 600 mm and mean air temperature of 9°C (Potthast et al., 2017).

Ten throughfall and four rainwater collectors with a sampling area of 314 cm^2 at approximately 1.2 m height were deployed at a forest and an open area plot 2 km apart, respectively (**Figure 1B**). Stemflow collars were installed at two tree individuals of each *F. sylvatica* and *A. pseudoplatanus* at 1.3 m height with a basal area in breast height between 346 to 740 cm^2. Rainwater, throughfall and stemflow plastic containers were cleaned and surface-disinfected with H_2O_2 prior to exposure and were placed in the field 1 to 2 days before two major rain events in May (expressed as early growing season) and September 2020 (expressed as late growing season), respectively. All three collector types were equipped with a 2 mm PE mash to avoid the introduction of large particles or insects during the collection period. Seepage was obtained from 16 zero-tension lysimeters with an area of 284 cm^2 accessing soil leachate which percolated the soil through the litter, and the upper 4 cm, 16 cm and 30 cm (Krüger et al., 2021). Details on lysimeter properties and installation were described by Potthast et al. (2017). Residual solution from the lysimeters was emptied before the rain events to obtain only freshly percolated soil leachate. Throughfall, stemflow and seepage solutions at the forest site and bulk rainwater at the pasture site were sampled on 13th May 2020 and 28th September 2020 after rain events of 12 mm falling within 24 h and 19 mm falling within 48 h, respectively

146 (**Figure 1C**). Triplicate leaf samples of the phyllosphere from two individuals of *F. sylvatica*
147 and *A. pseudoplatanus* at low canopy height of 4 to 5 m were clipped off with ethanol cleaned
148 scissors and stored in autoclaved plastic container after each rain event. In addition, soil
149 samples as reference to the mobilized microbial communities were collected in triplicates close
150 to the lysimeters at 0 to 4 cm, 4 to 16 cm and 16 to 30 cm depths in May 2020. All samples
151 were stored in cooling boxes at approximately 8°C during transport and were immediately
152 processed at the laboratory within 2 h. Rainwater, throughfall, stemflow, and seepage samples
153 were weighed to determine the volume and 10 to 100 ml was used for determination of pH,
154 electrical conductivity, carbon, nitrogen, and elemental analysis. For molecular analyses,
155 water samples were filtered through 0.2 µm polyethersulfone membrane filters (Supor, Pall
156 Corporation, USA) and stored at -80°C. Filtrate was stored at -20°C for determination of
157 inorganic nitrogen. Phyllosphere samples in plastic bottles were treated with 1 min of mild
158 sonification in 250 ml NaCl buffer (0.15 M NaCl + 0.1 % Tween 20) to detach microorganisms
159 from leaf surfaces, followed by 20 min shaking at 100 rpm (Herrmann et al., 2021). Resulting
160 suspensions were filtered through 0.2 µm pore size filters and stored at -80°C until further
161 processing. The remaining leaves were dried at 50°C for 1 week to measure the dry weight.
162 Soil samples for molecular analysis were stored at -80°C while those for determination of dry
163 weight and pH were stored at 4°C.

164 **2.2 Physicochemical analyses and calculation of matter fluxes**

165 Rainwater, throughfall, stemflow, and seepage samples were analyzed for total organic
166 carbon (TOC), inorganic carbon (IC) and total nitrogen (TN) as well as dissolved organic
167 carbon (DOC) and total dissolved nitrogen (TDN) concentrations (see Dataset 1). Analysis
168 involved filtration through <0.45 µm prewashed membrane filters (cellulose acetate, Sartorius,
169 Göttingen, Germany) for dissolved elements and catalytic thermal oxidation and
170 NDIR/chemiluminescence detection of both non-filtrated and filtrated samples using a TOC-
171 VCPN/TNM-1 (Shimadzu, Duisburg, Germany) (Potthast et al., 2017). Particulate organic
172 carbon (POC) and total particulate nitrogen (TPN) were calculated by subtracting the dissolved

173 fractions from the total concentrations. Inorganic nitrogen (IN), mainly consisting of NH_4^+ and
174 NO_3^- was determined by standard colorimetric approaches (Scheiner, 1974; Seelmeyer,
175 1954).

176 Fluxes of TOC, TN, IN, and IC per h of rain events were calculated from the concentration of
177 the respective parameters in the water samples (rainwater, throughfall, stemflow, seepage)
178 multiplied by the respective sample volume and the collector area and were expressed in mg
179 C or N m^{-2} h^{-1} as shown in Eq. 1 where C_s is the measured analyte concentration of a given
180 sample, V_s represents the collected water volume, A_c is the area of the particular sample
181 collector and t correspond to the rainfall period in h.

182 Eq. 1

183 $$flux = \left[(C_S \times V_S) \times \left(\frac{1}{A_C}\right)\right] / \, t$$

184 Stemflow fluxes were calculated for the individual basal area of each tree specimen and scaled
185 up to the tree stand area in m^2 per ha from both species.

186 Electrical conductivity and pH were determined using a WTW pH / Cond meter (pH Cond 3320
187 with SenTix81 and TetraCond, Weilheim, Germany) (Potthast et al., 2017). The soil water
188 content was determined by drying the samples over 48 h at 105°C. Soil pH was determined
189 from slurries prepared using sterile deionized water (ratio 1:2.5) and measured with a pH glass
190 electrode (Krüger et al., 2021).

191 **2.3 DNA extraction, quantitative PCR, and amplicon sequencing**

192 Microbial biomass from a filter half (leaves, rainwater, throughfall, stemflow, seepage) and
193 from 0.25 g of soil of each sample were extracted using the DNeasy PowerSoil kit (Qiagen,
194 Germany) following the manufacturer's protocol and stored at -20°C. Bacterial and archaeal
195 16S rRNA gene abundances were quantified with a CFX96 real-time PCR thermocycler (Bio-
196 Rad, USA) using primer pair Bakt_0341F/Bakt_799R (Klindworth et al., 2013, Chelius and
197 Triplett, 2001) which discriminates against chloroplast-derived 16S rRNA genes, and

198 Arch806F/Arch958R (DeLong, 1992; Takai and Horikoshi, 2000), respectively. Details on PCR
199 and cycling conditions are described elsewhere (Herrmann et al., 2021; Krüger et al., 2021).
200 Plasmids containing cloned bacterial and archaeal 16S rRNA gene fragments were used to
201 construct qPCR standards, which were linear across the concentration range of 50 to 5 $x10^8$
202 copies per reaction. Gene abundances in rain, throughfall, stemflow and seepage were
203 calculated as per L, while gene abundance on leaf surfaces and soil was expressed as genes
204 per g of dry weight (see Dataset 1).

205 Library construction for 16S rRNA gene targeted amplicon sequencing assessing the bacterial
206 community composition across samples was conducted with the same primer pair as for
207 qPCR, targeting the V3-V4 region of the bacterial 16S rRNA gene. Reactions were performed
208 with 1 ng DNA template per sample in 15 µl volume reactions under previously reported
209 conditions (Herrmann et al., 2021). Subsequent steps are described in Krüger et al. (2021),
210 and sequencing was performed on an Illumina MiSeq platform using v3 chemistry.

211 **2.4 Sequence processing**

212 PCR primer sequences were trimmed from raw reads using Cutadapt (Martin, 2011) and reads
213 were further processed with the R package DADA2 1.22.0 following the standard sequence
214 analysis pipeline for 16S rRNA genes (Callahan et al., 2016). Trimmed reads were filtered and
215 denoised using the filterAndTrim function under the following conditions: (truncLen = c(270,
216 240), maxEE = c(2,3), truncQ = 2, maxN = 0). The filtered reads of each sample were
217 dereplicated, Amplicon Sequencing Variants (ASVs) were deduced for forward and reverse
218 reads separately, and then the forward and reverse reads were merged at overlapping
219 positions. Chimeric sequences were removed and taxonomic assignment of amplicon
220 sequence variants (ASV) was performed using the SILVA taxonomy reference database
221 release version 138 (Quast et al., 2013). Subsequent sequence analysis was conducted using
222 the package phyloseq (McMurdie and Holmes, 2013) and is further described in the
223 Supplementary Methods.

224 **2.5 Prediction of microbial functions**

225 To approximate the functional potential of the microbial communities across the different
226 compartments, PICRUSt2 (Phylogenetic Investigation of Communities by Reconstruction of
227 Unobserved States) analysis was applied to predict microbial functions based on the obtained
228 amplicon sequencing data using v2.3.0 beta following the standard procedure for 16S rRNA
229 (Douglas et al., 2020). ASV sequences were first aligned and placed into a reference tree and
230 ASVs were corrected for multiple 16S rRNA genes by the 16S rRNA operon number of closely
231 related representatives. Gene families for each ASV were predicted based on KEGG orthologs
232 (KO) as identifiers for metabolic pathways (Kanehisa et al., 2023). The PICRUSt2 output of
233 7,523 KOs was subset for KO abundance of enzymes involved in the following pathways:
234 carbon fixation, nitrogen fixation, methane oxidation, carbon degradation and protein
235 hydrolysis (see Dataset 4). Metagenomic predictions of the selected pathways were based on
236 the relative abundance of the KO IDs across each sample. To assess the proportion of the
237 bacterial community associated with the selected metabolic functions across samples, we
238 used the relative abundance of each ASV from amplicon sequencing data for which a
239 corresponding KO was predicted (see Dataset 4).

240 **2.6 Determination of absolute cell abundances and cell fluxes**

241 Studies have shown that combining amplicon sequencing of marker genes and qPCR can be
242 used as an accurate method to infer cell numbers similar to direct cell determination by flow
243 cytometry (Bittar et al., 2018) and to enhance bacterial community profiling (Jian et al., 2020).
244 The quantity of exported cells was calculated using the 16S rRNA qPCR-based gene
245 abundances per liter and the amplicon sequencing reads on family-level (see Dataset 2). To
246 account for diverging operon numbers of the 16S rRNA gene across the 303 observed
247 bacterial families, gene abundances were corrected using the number of operons of the
248 respective family-level taxa obtained from the ribosomal RNA operon database
249 (https://rrndb.umms.med.umich.edu/) (Stoddard et al., 2015) (see Dataset 3). The estimated
250 total cell abundance per liter (T_{abs}) for each sample of rainwater, throughfall, stemflow and

seepage was determined based on the relative read abundance from each taxon divided by the family-specific operon numbers and multiplied by the total 16S rRNA gene abundance. This calculation is expressed in Eq. 2 where S_{abs} represents the total gene abundance of a given sample, T_{rel} is the relative abundance of a taxon and T_n represents the number of 16S rRNA operons for a taxon.

Eq. 2

$$T_{abs} = S_{abs} \times (T_{rel} \,/\, T_n)$$

Bacterial cell fluxes per m^2 h^{-1} were calculated as described for TOC and TN using the estimated absolute cell abundance per total sample volume and collector area for each sample, divided by the duration of the respective rain event (see Dataset 1).

2.7 Estimation of bacterial contributions to TOC and TN

The fraction of bacterial cell carbon and nitrogen contributing to TOC and TN in rainwater, throughfall, stemflow and seepage was estimated as previously described (Herrmann et al., 2023; Krüger et al., 2021). Briefly, a mean carbon content of 39 fg per cell and mean nitrogen content of 12 fg per cell was assumed as estimated under carbon-limited and nitrogen-limited conditions (Vrede et al., 2002), respectively. The contribution of bacterial cell carbon and nitrogen to TOC and TN, respectively, was estimated by first multiplying the operon number corrected absolute bacterial abundances as well as the TOC/ TN content per liter by the sample volume. The estimated number of bacterial cells was multiplied by the assumed carbon and nitrogen content per cell. The resulting estimates of microbial cell carbon and nitrogen were then set in relation to the total organic carbon (TOC) and total nitrogen (TN) in the corresponding samples to estimate the bacterial contribution (Dataset 3).

2.8 Statistical analysis

All statistical tests were performed using R version 4.1.2 (R Core Team, 2020) unless otherwise described. Normal distribution of gene abundances and element fluxes were tested with Shapiro-Wilk test. Non-parametric Kruskal-Wallis rank sum test and Dunn's multiple

comparison post-hoc test with R package FSA (Ogle et al., 2020) was used to test data for significant differences between the compartments. Nonmetric multidimensional scaling using Bray-Curtis distance matrix was performed to test dissimilarity of the bacterial community between the compartments, the growing seasons and the tree species. More details on statistical methods and the R packages used are provided as Supplementary Methods.

282 # 3. Results

283 ## 3.1 Carbon and nitrogen fluxes across compartments

284 The export of total organic carbon (TOC) ranged from 0.1 mg C m^{-2} h^{-1} in stemflow to 45.1 mg
285 C m^{-2} h^{-1} in seepage right below the litter layer and was significantly different between
286 compartments ($p < 0.001$) (**Figure 2A**). Inorganic carbon (IC) fluxes were on average 2 to 4
287 times lower across all compartments (**Figure S 1**). Total nitrogen (TN) flux varied from as low
288 as 0.01 mg N m^{-2} h^{-1} in stemflow to a maximum of 29.3 mg N m^{-2} h^{-1} in seepage collected
289 after percolation through the upper 16 cm of the soil profile (**Figure 2A**). C:N ratios showed
290 significantly higher values in throughfall and stemflow ($p < 0.001$) compared to rainwater and
291 seepage (**Figure S 1**). Ammonium flux decreased from rainwater, throughfall and stemflow to
292 the seepage flow path while fluxes of nitrate were highest in seepage (**Figure S 1**).

293 ## 3.2 Microbial gene abundances, estimated cell fluxes, and contributions to C
294 ## and N transport across compartments

295 Bacterial 16S rRNA gene abundances per L (**Figure S 2**A) differed significantly between the
296 different compartments ($p < 0.001$) and were highest in throughfall and stemflow. Rainwater
297 exhibited on average three orders of magnitude lower gene abundances. In seepage, bacterial
298 16S rRNA gene abundances decreased with increasing collection depth from below the litter
299 layer down to 30 cm soil depth. Archaeal 16S rRNA gene abundances were consistently two
300 to three orders of magnitude lower than bacterial 16S rRNA gene abundances and exhibited
301 an opposing depth-dependent trend in seepage.

302 We further estimated bacterial cell abundances per g and L based on qPCR data and amplicon
303 sequencing data, applying family-level corrections for multiple 16S rRNA gene operons per
304 cell (**Table S 1**). Estimated bacterial abundances on leaf surfaces ranged from 1.4 x 10^5 to 5.4
305 x 10^8 cells g^{-1} dry leaf material while soil bacterial abundances ranged from 9.6 x 10^8 to 7.8 x
306 10^9 cells g^{-1} dry soil. In rainwater, estimated bacterial cell abundance ranged from 1.2 x 10^6 to
307 1.6 x 10^8 cells L^{-1} while throughfall and stemflow cell abundances were about 100 times

308 higher, ranging from 5.8 x 10^8 to 3.1 x 10^{11} cells L^{-1} and 7.9 x 10^9 to 2.3 x 10^{11} cells L^{-1},
309 respectively. Seepage bacterial abundance ranged from 3.8 x 10^8 to 3.9 x 10^{10} cells L^{-1} with
310 a decreasing trend with soil depth ($p < 0.01$).

311 Based on estimated cell abundances, we also determined the flux of bacterial cells per m^2 and
312 h transported by rain, throughfall, stemflow and seepage during both sampling events. Across
313 all samples and the two sampling time points, cell fluxes ranged from lowest values in
314 rainwater with 4.7 x 10^5 cells m^{-2} h^{-1}, 1.9 x 10^{10} cells m^{-2} h^{-1} by seepage from the litter layer to
315 highest export of 1.0 x 10^{11} cells m^{-2} h^{-1} by throughfall with significant differences between
316 compartments ($p < 0.001$) (**Figure 2A**). On average, cell fluxes via throughfall and litter layer
317 were three orders of magnitude higher than in rainwater. Seepage-mediated cell fluxes of
318 seepage collected below 4 cm soil depth were one order of magnitude lower than in
319 throughfall. No differences in estimated cell fluxes were observed between early and late
320 growing season for a given compartment.

321 Fluxes of TOC and TN by rainwater, throughfall and seepage were positively correlated with
322 the estimated total bacterial cell flux across all compartments and sampling months ($p < 0.05$)
323 (**Figure 2B**), underlining the strong relationship between microbial transport dynamics and
324 matter transport. Estimation of the bacterial contribution to matter transport indicated a
325 significant bacterial contribution across the different water flow pathways ($p < 0.001$) with
326 bacterial cells contributing between 0.006 % of TOC and 0.007 % TN in rainwater, and up to
327 11.3 % TOC and 33.6 % TN in throughfall **(Figure 2A)**.

328 **3.3 Bacterial community composition from phyllosphere to soil**

329 The ASV richness and alpha diversity (Shannon index) differed significantly between all
330 compartments (Kruskal-Wallis, $p < 0.001$) (**Figure 3A**). The highest number of different
331 bacterial taxa was observed in seepage, followed by stemflow, soil, leaf surface and
332 throughfall samples, while rainwater samples were the least diverse. Leaf, seepage, and soil
333 communities were on average more diverse than communities from rain, throughfall and
334 stemflow samples ($p < 0.05$). Alpha diversity and species richness of throughfall and stemflow

335 communities were lower during early growing season compared to late growing season ($p <$
336 0.05) while this effect was not observed for the other compartments.

337 Beta diversity analysis of bacterial communities revealed a clear differentiation based on the
338 sampled compartment (ANOSIM, $R^2 = 0.52$, $p < 0.001$) with phyllosphere, seepage and soil
339 communities being distinct, while rainwater, throughfall and stemflow communities appeared
340 very variable and were not clearly separated (**Figure 3B**). The compartment was the strongest
341 driver for community differentiation, accounting for 25.2 % of the total community variation
342 (PERMANOVA, $p < 0.001$) (**Figure 3B**). The sampling month contributed 2.1 % of the
343 variation. The influence of tree species (European beech versus sycamore maple) explained
344 only less than 1 % of the variation and was not included as an influencing factor in further
345 analysis.

346 On family-level, 23 bacterial taxa comprised each more than 1 % of the total community
347 (**Figure S 2**B), which exhibited distinct distribution patterns across rain, throughfall, stemflow
348 and seepage (ANOSIM: $R^2 = 0.54$, $p < 0.001$). Gammaproteobacteria, Alphaproteobacteria,
349 Bacteroidia, Actinobacteria and Acidobacteriae accounted for at least 90 % of all sequence
350 reads across all samples (**Figure 3C**). Across rainwater, throughfall and stemflow samples,
351 *Pseudomonadaceae* accounted for a large proportion of between 24 – 42 % together with
352 common plant pathogens such as *Erwiniaceae* and *Yersiniaceae*, particularly during the early
353 growing season. In phyllosphere samples, *Hymenobacteraceae* (32 mean ± 7 % standard
354 deviation) dominated at the late growing season sampling point together with
355 *Sphingomonadaceae* (16 ± 7 %) while *Beijerinckiaceae* (13 ± 6 %) were more abundant at the
356 early growing season. In contrast to rainwater, throughfall and stemflow,
357 Gammaproteobacteria were less abundant in phyllosphere samples and were here mostly
358 represented by *Oxalobacteraceae* (5 ± 3 %) and *Comamonadaceae* (6 ± 4 %) in the early and
359 late growing season samples, respectively. In soil communities, Alphaproteobacteria
360 accounted on average for 24 ± 3 % with *Xanthobacteraceae* being the dominant family (19 ±

361 3 %). Seepage communities were dominated by *Flavobacteriaceae, Oxalobacteraceae* and
362 *Comamonadaceae*.

363 The taxonomic composition derived from estimated cell abundances confirmed the patterns
364 revealed by relative read abundances (**Figure S 2**C). Analysis based on absolute abundance
365 revealed that most of rainwater-derived bacterial families, including *Pseudomonadaceae*,
366 *Yersiniaceae* and *Sphingomonadaceae*, were two to five orders of magnitude more abundant
367 in throughfall and stemflow. In contrast to those communities, the bacteria in seepage depicted
368 a two to three orders of magnitude increase in cell abundance of taxa such as
369 *Xanthobacteraceae*, *Spirosomaceae* and *Diplorickettsiaceae,* which showed also high relative
370 abundances in soil communities.

371 **3.4 Predicted functions of bacterial communities**

372 The prediction of the bacterial genetic repertoire for selected biogeochemical transformations
373 unveiled distinct patterns across the compartments (**Figure S 3**, ANOSIM: $R^2 = 0.42$, $p <$
374 0.001). The predicted relative abundance of KOs showed that most pathways had higher
375 prevalence towards soil and leaf communities except for protein hydrolysis, which was more
376 prevalent in bacteria transported by seepage.

377 The functional metagenomic prediction was based on the presence and absence of functional
378 modules of each pathway (**Figure 4A**). Hydrolytic enzymes showed high relative abundances
379 of methionyl aminopeptidase (0.083 %) and leucyl aminopeptidase (0.062 %) across the
380 samples. Potential for the degradation of carbon sources was also highly prevalent across the
381 samples depicted by beta-N-acetylhexosaminidase (0.046 %), hexosaminidase (0.033 %),
382 beta-glucosidase (0.029 %), chitinase (0.022 %) and alpha-amylase (0.017 %). Potential for
383 carbon fixation was mostly associated with the Calvin–Benson–Bassham pathway,
384 represented by *cbbS* and *cbbL* genes with an average relative abundance of 0.002 % and
385 0.006 %. Nitrogenases as primary enzymes for nitrogen fixation were prevalent in soil (0.0037
386 %), phyllosphere (0.0022 %) and seepage communities (0.0018 %). Methane oxidation was

primary related to methanol dehydrogenase (0.0014 %) across all samples, with the highest relative fraction in phyllosphere (0.0037 %) and rainwater communities (0.0024 %).

A similar pattern of the functional profiles across the compartments was observed based on relative abundance of bacterial classes for which predicted KO were present (**Figure 4B**). The prevalence of bacteria which showed functional potential differed significantly between the compartments for each pathway ($p < 0.05$). The fraction of bacterial communities showing capability of utilizing enzymes involved in various carbon and protein decomposition processes ranged, on average, from 52 % in throughfall to 75 % in seepage and 60 % in throughfall to 80 % in leaf samples, respectively. Carbon fixation made up by a fraction of 2 % to 13 % of the bacterial community with lowest potential in throughfall and stemflow, and highest potential in seepage samples. Pathways related to biological nitrogen fixation and methane oxidation showed the highest prevalence of 2.5 % and 1.1 %, respectively, in leaf communities, while rain and throughfall communities showed functional potential for both pathways of less than 1 %.

3.5 Association of bacterial taxa with rainwater- and seepage-driven transport

Only a small proportion of 0.19 % (23 ASVs from a total of 12191 ASVs without singletons) of the bacterial community was shared across all compartments. These shared ASVs were especially abundant in the communities that were transported by rainwater, throughfall or stemflow, with ASVs related to *Pseudomonas*, *Massilia* and *Sphingomonas* accounting for up to 33% of sequence reads in the respective communities (Figure S 4). The major fraction of 62 % of all ASVs observed in this study were exclusively present in seepage, while less than 10 % of the total ASVs were only found in either rain, throughfall or stemflow communities. Stemflow communities shared 5.9 % of the ASVs with rainwater, 10.7 % with throughfall, and 6.9 % with seepage.

We defined bacterial core taxa based on occurrence in at least 70 % of all samples and tracked the increase or decline of single core ASVs across the different compartments, along with an assessment of their potential transport by throughfall, stemflow, and seepage. Core taxa which

414 constituted a large community fraction on leaves included members of the
415 *Hymenobacteraceae*, *Acetobacteraceae*, *Bejierinckiaceae* and *Sphingomonadaceae*. ASVs
416 affiliated with the genera *Hymenobacter*, *Acidiphilium*, *Methylorubrum* and *Sphingomonas*
417 accounted for up to 1 % relative abundance of the total community on leaves but were less
418 abundant in rainwater. Some ASVs classified as *Sphingomonas* were also observed in
419 throughfall and stemflow (**Figure 5**, **Figure S4**). Among the phyllosphere community,
420 *Acidiphilium*, *Methylorubrum* and *Sphingomonas* were also observed in rainwater.-In contrast,
421 *Pseudomonadaceae* and *Oxalobacteraceae* including the genera *Pseudomonas* and
422 *Massilia*, respectively, were abundant in rainwater, contributed on average 41% ± 24% and
423 14% ±11% of the communities in throughfall and 42% ± 30% and 13% ±8% in stemflow, but
424 were less abundant in seepage with 3.3% ± 3.7% and 3.6% ± 2.8% and on leaves (3% ± 5.2%
425 and 3.3% ± 2.8%, respectively).

426 In addition to the preferential association of core ASVs with a specific compartment, we
427 determined the differential abundance of genus-level taxa which showed either the tendency
428 to stick on leaf surfaces or to be washed off by throughfall and stemflow (**Figure S 5**),
429 indicating their potential to become subject to rainwater-mediated transport. Members of
430 *Pseudomonadaceae*, *Yersiniaceae* and *Oxalobacteraceae* exhibited high relative
431 abundances in throughfall and stemflow while *Sphingomonadaceae* and *Hymenobacteraceae*
432 showed stronger association with the phyllosphere. Instead, members of *Xanthobacteraceae*
433 and *Flavobacteriaceae* showed higher relative abundances in seepage compared to
434 throughfall and stemflow (**Figure S 6**), and *Flavobacteriaceae* and *Sphingomonadaceae*
435 formed a larger fraction of the seepage community compared to soil. LEFSe analysis
436 confirmed the specific association of those bacterial taxa with either the tree phyllosphere or
437 rainwater-, throughfall- or stemflow-associated mobilized fractions (**Figure S 7**).

438 # 4. Discussion

439 Precipitation events transmit a vast number of organic particles, including microbes,
440 representing a major environmental agent connecting the atmosphere with the phyllosphere,
441 pedosphere and lithosphere (Ponette-González et al., 2020; Van Stan et al., 2020). The
442 transported matter and microbial cells can potentially impact microbial communities and
443 nutrient cycling along the water flow path from the plant phyllosphere to soil (Van Stan and
444 Stubbins, 2018; Van Stan et al., 2020). However, the extent of rainwater-driven microbial
445 mobilization within the forest phyllosphere and from bark surfaces, and its contribution to
446 carbon and nitrogen fluxes have so far remained unknown. Here, we assessed the diversity
447 and abundance of bacteria along this flow path, starting from intercepting rain via tree canopy-
448 derived throughfall and stemflow to soil seepage in a temperate forest area at an early and
449 late stage of the growing season.

450 Our results clearly demonstrate that canopy-derived throughfall and stemflow microbial
451 communities are quantitatively important carriers of organic matter to the forest floor,
452 contributing up to 11 and 34 % to total carbon and nitrogen fluxes, respectively. Thus, they
453 play a central role in the throughfall- and stemflow-mediated provision of fresh organic carbon
454 and nitrogen to the forest floor (Van Stan et al., 2021). Throughfall and stemflow obtained in
455 this study from a beech forest during a two-days rain event were highly enriched with bacteria
456 with 10 to 1000 times higher estimated cell numbers than previously reported from a
457 subtropical oak-cedar forest (Bittar et al., 2018). Given the fact that throughfall and stemflow
458 samplers were directly sampled at the end of a three-days exposure period at overall low
459 ambient temperatures between 0-20°C, we can exclude that massive growth of bacterial cells
460 in the samplers may have led to a strong overestimation of these bacterial loads. Despite on
461 average similar cell concentrations L^{-1} in throughfall and stemflow solutions, stemflow-
462 mediated cell fluxes normalized to tree stand area and h were two orders of magnitude lower
463 than in throughfall, which is typically also observed for TOC and TN fluxes when comparing
464 these two water flow paths (Van Stan and Stubbins, 2018). Throughfall cell fluxes were

comparable to those from seepage collected below the litter layer, indicating a substantial above-ground translocation of bacteria to soil.

In contrast to the high estimated proportions of bacterial derived carbon and nitrogen in throughfall and stemflow, bacterial contributions to TOC and TN were three times lower in seepage solutions, matching with previously reported values from the same lysimeters (Krüger et al., 2021) and tension-controlled lysimeters from the same field site (Herrmann et al., 2023). Total estimated cell fluxes were even ten times lower in seepage below 16 cm compared to throughfall. Apparently, a large fraction of the cells mobilized by throughfall and stemflow get retained in the soil, which acts as a strong filter for this above-ground transport. Turnover processes in the soil result in carbon and nitrogen export primarily as dissolved compounds with a lower contribution of mobilized microbial cells. During rain events, throughfall and stemflow mediated inputs might supplement the nutrient pool of the forest litter and soil and could additionally affect microbial nutrient cycling capabilities by introducing active microorganisms with their respective biodegradation capabilities or exoenzymes from upstream communities. Pathway predictions indeed indicated that bacterial communities from throughfall, stemflow and seepage exhibited strong potential for hydrolytic degradation of carbohydrates and proteins. However, since PICRUSt2 only predicts metagenomic functions from marker gene abundance and phylogenetic placement to reference sequences (Douglas et al., 2020), speculations about the full degradation potential need to be treated with caution.

The type of canopy-derived transport agent (throughfall versus stemflow) was the strongest effector for bacterial community similarity/ dissimilarity, suggesting that the composition of the phyllosphere versus bark-associated source communities and potential differences in microbial detachment mechanisms between these two habitats could underlie the observed community differences. Phyllosphere communities were more similar to rain, throughfall and stemflow communities than to seepage and soil, suggesting an exchange of microbes between phyllosphere, throughfall and stemflow in a taxon-specific manner. Rainwater can potentially support the colonization but also the wash-off of epiphytic microbes from leaf

surfaces (Guerrieri et al., 2020). The observed fraction of 10 % of shared ASVs between throughfall and stemflow communities suggested that runoff from the canopy exported a basic, selective fraction of bacteria independent of the phyllosphere location, which was further modulated by exchange with the specific colonizers of either leaves or bark (Guerrieri et al., 2020; Teachey et al., 2018). Similarly, Hudson et al. (2023) demonstrated that the bacterial community composition in stemflow was distinct from that found on tree bark. Bark-water interactions during rainfall may lead to the detachment of loosely attached microbes and enable their accumulation further down as infiltration source in soil (Carlyle-Moses et al., 2020).

Weather conditions and tree species were identified as important factors shaping throughfall bacterial communities in a mediterranean holm oak forest (Guerrieri et al., 2020) and a subtropical Southern live oak forest (Teachey et al., 2018) with Alphaproteobacteria, Gammaproteobacteria and Bacteroidia representing main bacterial classes. Following the above-ground flow path at our study site, phyllosphere-inhabiting *Pseudomonadaceae*, *Erwiniaceae*, *Oxalobacteraceae* and *Sphingobacteriaceae* may partially have originated from rainfall-mediated atmospheric inputs of early leave colonizers and exhibited 10 to 100 times higher relative abundances on leaf surfaces compared to rainwater. In turn, they also appeared to be selectively transported by throughfall and stemflow, indicating an overall high mobilization potential of these taxa. Our results further demonstrated a substantial difference in the microbial communities of the above-ground flow paths – rainwater, throughfall and stemflow - when comparing an early and late time point of the growing season. During May sampling, *Pseudomonadaceae* accounted on average for over 50 % of the total community in bulk rain, throughfall and stemflow, indicating that at this time point, only a single taxonomic group contributed substantially to matter transport and potential carbon degradation capabilities. *Pseudomonas* species act as common pathogens and epiphytic plant commensals in the phyllosphere (Vorholt, 2012). However, they are also typically observed among microbes attached to plant pollen (Manirajan et al., 2018), which can be transmitted

519 by dry deposition (Sánchez-Parra et al., 2021) and rainwater (Cho and Jang, 2014). Higher
520 pollen bioaerosols or pollen deposits derived from the flowering of beech or nearby Norway
521 spruce stands in May might have constituted a large microbial source of pollen-associated
522 *Pseudomonadaceae* in rainwater, throughfall and stemflow (Guidone et al., 2021).

523 The observed distinction of bacterial communities in seepage versus throughfall and stemflow
524 may not only be linked to differences in the bacterial source communities but also to
525 differences in the general bacterial detachment mechanisms between above-ground and
526 below-ground habitats. Preferential, taxon-specific microbial transport through soil by
527 seepage-mediated translocation is mainly attributed to cellular characteristics such as cell
528 size, shape and surface charge (i.e., zeta potential) (Dibbern et al., 2014; Herrmann et al.,
529 2023). In the phyllosphere, the main factor controlling the preferential transfer from leaf
530 surfaces to throughfall might be the strength of attachment to the surface rather than cell size.
531 Members of the *Pseudomonadaceae* can increase local water availability of leaf surfaces by
532 releasing surfactants, allowing proliferation (Koskella, 2020), which might also be a reason for
533 preferential mobilization and detachment of members of this family by throughfall and
534 stemflow. In addition, surfactants may also support the detachment of other leaf-associated
535 microorganisms. Prevalent bacterial epiphytes from the phyllosphere beyond
536 *Pseudomonadaceae* are *Beijerinckiaceae* and *Sphingomonadaceae* (Delmotte et al., 2009;
537 Vorholt, 2012), which were also observed in throughfall and stemflow at our study site.
538 Especially *Pseudomonadaceae* could also constitute an important source of extracellular
539 exoenzymes performing hydrolytic degradation, affecting decomposition of organic matter
540 (Mori et al., 2019).

541 Despite the high numbers of cells transported by throughfall and stemflow, it remains an open
542 question whether cells remain viable throughout the whole vertical passage, and how many
543 living microbes ultimately reach the soil. A seepage study using electron microscopy indicated
544 that living microbes remained intact during soil passage across 60 cm depth by seepage
545 transmission (Dibbern et al., 2014). However, it is unclear whether the throughfall- and

546 stemflow-mediated cell transfer to the soil mainly contributes to inputs of organic carbon and
547 nitrogen, or whether it adds to the functional potential and enzymatic capacity of the local soil
548 microbial populations.

549 Our results further suggest that multiple taxa were able to colonize and thrive in all of the
550 investigated ecosystem compartments from atmosphere to soil. Establishment and
551 proliferation in the respective compartments probably ensure that the taxa can also be
552 released again from these compartments and be transported by throughfall, stemflow or
553 seepage. However, with our approach, we cannot distinguish between continuous cross-
554 compartment transport of individual cells or discontinuous transport, resulting from
555 establishment in each compartment, proliferation, and subsequent secondary mobilization of
556 microbial taxa. Consequently, occurrence of the same ASVs across the vertical flow path does
557 not necessarily indicate an uninterrupted flow of individual cells through the system but the
558 ability of certain taxa to be continuously mobilized from one compartment and transported to
559 the other, and to establish stable populations in the respective sink communities, from
560 whereon cells can be mobilized again, resulting in the observed overlaps of microbial
561 communities and their functional potential between neighboring ecohydrological
562 compartments.

563 5. Conclusion

564 Our study clearly demonstrates that microorganisms transported by rainwater, throughfall,
565 stemflow and seepage contribute substantially to carbon and nitrogen fluxes in a deciduous
566 forest ecosystem. Contributions and cell fluxes were larger in above-ground compared to
567 below-ground compartments, suggesting that a considerable fraction of mobilized cells was
568 retained in the soil and not further transported. Throughfall- and stemflow-mediated flow paths
569 act as substantial carriers of microbial biomass, carbon and nitrogen which might affect soil
570 matter transformation by introducing a fresh source of nutrients and energy but also new
571 genetic variability to the respective microbial sink communities. In contrast to periodic cell and
572 nutrient inputs via litter fall, the throughfall- and stemflow-mediated vertical microbial transport

to the forest floor takes place throughout the year, acting as central connection between phyllosphere and forest floor in terms of carbon and nitrogen inputs but also as contribution to the functional diversity of soil microbiomes. Our results further expand a previously observed taxon-specificity in seepage-mediated microbial mobilization in soil to throughfall and stemflow, presumably along with different mechanisms of microbial detachment across these flow paths.

Data availability

Raw sequence files were deposited at the European Nucleotide Sequence Archive with project number PRJEB92466 under accessions ERS25231161 to ERS25231303.

Acknowledgements

We thank Falko Gutmann, Stefan Riedel and Linda Gorniak for support of field and laboratory work, and Martin Stephan from the Otto Schott Institute for Materials Research at Friedrich Schiller University Jena for producing customized soil lysimeters. We are further grateful for the background graphics provided by Clemens Schulze.

Funding

This study was part of the Collaborative Research Centre 1076 AquaDiva (CRC AquaDiva) of the Friedrich Schiller University Jena, funded by the Deutsche Forschungsgemeinschaft under project number 218627073. The infrastructure for MiSeq Illumina sequencing was financially supported by the Thüringer Ministerium für Wirtschaft, Wissenschaft und Digitale Gesellschaft (TMWWDG project 2016 FGI 0024 “BIODIV”).

Author contributions: CRediT

Markus Krüger: Conceptualization, Formal analysis, Investigation, Methodology, Visualization, Writing – original draft, Writing – review and editing. **Karin Potthast**: Conceptualization, Methodology, Writing – review and editing. **Beate Michalzik**: Conceptualization, Writing – review and editing. **Alexander Tischer**: Conceptualization, Methodology, Writing – review and editing. **Martina Herrmann**: Funding acquisition, Conceptualization, Sample processing, Writing – review and editing.

Declaration of competing interest

The authors declare that the work of this study was achieved without financial or personal conflict of interest.

References

Andrews, J.H., Harris, R.F., 2000. The ecology and biogeography of microorganisms on plant surfaces. Annu. Rev. Phytopathol. 38, 145-180. https://doi.org/10.1146/annurev.phyto

Bittar, T.B., Pound, P., Whitetree, A., Moore, L.D., Van Stan, J.T., 2018. Estimation of Throughfall and Stemflow Bacterial Flux in a Subtropical Oak-Cedar Forest. Geophys. Res. Lett. 45, 1410–1418. https://doi.org/10.1002/2017GL075827

Callahan, B.J., McMurdie, P.J., Rosen, M.J., Han, A.W., Johnson, A.J.A., Holmes, S.P., 2016. DADA2: High-resolution sample inference from Illumina amplicon data. Nat. Methods 13, 581–583. https://doi.org/10.1038/nmeth.3869

Carlyle-Moses, D.E., Iida, S., Germer, S., Llorens, P., Michalzik, B., Nanko, K., Tanaka, T., Tischer, A., Levia, D.F., 2020. What We Know About Stemflow's Infiltration Area. Front. For. Glob. Chang. 3. https://doi.org/10.3389/ffgc.2020.577247

Chelius, M.K., Triplett, E.W., 2001. The diversity of archaea and bacteria in association with the roots of *Zea mays* L. Microbial Ecol 41: 252-263. https:// doi: 10.1007/s002480000087

Cho, B.C., Jang, G. Il, 2014. Active and diverse rainwater bacteria collected at an inland site in spring and summer 2011. Atmos. Environ. 94, 409–416. https://doi.org/10.1016/j.atmosenv.2014.05.048

Delmotte, N., Knief, C., Chaffron, S., Innerebner, G., Roschitzki, B., Schlapbach, R., Von Mering, C., Vorholt, J.A., 2009. Community proteogenomics reveals insights into the physiology of phyllosphere bacteria. Proc. Natl. Acad. Sci. U. S. A. 106, 16428–16433. https://doi.org/10.1073/pnas.0905240106

DeLong, E.F., 1992. Archaea in coastal marine environments. Proc. Natl. Acad. Sci. 89, 5685–5689. https://doi.org/10.1073/pnas.89.12.5685

Deng, Q., Hui, D., Chu, G., Han, X., Zhang, Q., 2017. Rain-induced changes in soil CO2 flux and microbial community composition in a tropical forest of China. Sci. Rep. 7, 5539. https://doi.org/10.1038/s41598-017-06345-2

Després, V.R., Alex Huffman, J., Burrows, S.M., Hoose, C., Safatov, A.S., Buryak, G., Fröhlich-Nowoisky, J., Elbert, W., Andreae, M.O., Pöschl, U., Jaenicke, R., 2012. Primary biological aerosol particles in the atmosphere: A review. Tellus, Ser. B Chem. Phys. Meteorol. 64, 15598. https://doi.org/10.3402/tellusb.v64i0.15598

Dibbern, D., Schmalwasser, A., Lueders, T., Totsche, K.U., 2014. Selective transport of plant root-associated bacterial populations in agricultural soils upon snowmelt. Soil Biol. Biochem. 69, 187–196. https://doi.org/10.1016/j.soilbio.2013.10.040

Douglas, G.M., Maffei, V.J., Zaneveld, J.R., Yurgel, S.N., Brown, J.R., Taylor, C.M., Huttenhower, C., Langille, M.G.I., 2020. PICRUSt2 for prediction of metagenome functions. Nat. Biotechnol. 38, 685-688. https://doi.org/10.1038/s41587-020-0548-6

Guerrieri, R., Lecha, L., Mattana, S., Cáliz, J., Casamayor, E.O., Barceló, A., Michalski, G., Peñuelas, J., Avila, A., Mencuccini, M., 2020. Partitioning between atmospheric deposition and canopy microbial nitrification into throughfall nitrate fluxes in a Mediterranean forest. J. Ecol. 108, 626–640. https://doi.org/10.1111/1365-2745.13288

Guidone, M., Gordon, D.A., Van Stan, J.T., 2021. Living particulate fluxes in throughfall and stemflow during a pollen event. Biogeochemistry 153, 323–330. https://doi.org/10.1007/s10533-021-00787-7

Herrmann, M., Geesink, P., Richter, R., Küsel, K., 2021. Canopy Position Has a Stronger Effect than Tree Species Identity on Phyllosphere Bacterial Diversity in a Floodplain Hardwood Forest. Microb. Ecol. 81, 157–168. https://doi.org/10.1007/s00248-020-01565-y

Herrmann, M., Lehmann, K., Totsche, K.U., Küsel, K., 2023. Seepage-mediated export of bacteria from soil is taxon-specific and driven by seasonal infiltration regimes. Soil Biol. Biochem. 187, 109192. https://doi.org/10.1016/J.SOILBIO.2023.109192

Hu, W., Niu, H., Murata, K., Wu, Z., Hu, M., Kojima, T., Zhang, D., 2018. Bacteria in atmospheric waters: Detection, characteristics and implications. Atmos. Environ. 179, 201-221. https://doi.org/10.1016/j.atmosenv.2018.02.026

Hudson, J.E., Levia, D.F., Yoshimura, K.M., Gottel, N.R., Hudson, S.A., Biddle, J.F., 2023. Mapping bark bacteria: initial insights of stemflow-induced changes in bark surface phyla. Microbiol. Spectr. 11, e03562-23. https://doi.org/10.1128/spectrum.03562-23

Jeffrey, L.C., Maher, D.T., Chiri, E., Leung, P.M., Nauer, P.A., Arndt, S.K., Tait, D.R., Greening, C., Johnston, S.G., 2021. Bark-dwelling methanotrophic bacteria decrease methane emissions from trees. Nat. Commun. 12, 2127. https://doi.org/10.1038/s41467-021-22333-7

Jian, C., Luukkonen, P., Yki-Järvinen, H., Salonen, A., Korpela, K., 2020. Quantitative PCR provides a simple and accessible method for quantitative microbiota profiling. PLoS One 15, e0227285. https://doi.org/10.1371/journal.pone.0227285

Kanehisa, M., Furumichi, M., Sato, Y., Kawashima, M., Ishiguro-Watanabe, M., 2023. KEGG for taxonomy-based analysis of pathways and genomes. Nucleic Acids Res. 51, 587–592. https://doi.org/10.1093/nar/gkac963

Klindworth, A., Pruesse, E., Schweer, T., Peplies, J., Quast, C., Horn, M., Glöckner, F.O., 2013. Evaluation of general 16S ribosomal RNA gene PCR primers for classical and next-generation sequencing-based diversity studies. Nucleic Acids Res. 41, e1. https://doi.org/10.1093/nar/gks808

Koskella, B., 2020. The phyllosphere. Curr. Biol. 30, 1143-1146. https://doi.org/10.1016/j.cub.2020.07.037

Krüger, M., Potthast, K., Michalzik, B., Tischer, A., Küsel, K., Deckner, F.F.K., Herrmann, M., 2021. Drought and rewetting events enhance nitrate leaching and seepage-mediated translocation of microbes from beech forest soils. Soil Biol. Biochem. 154, 108153. https://doi.org/10.1016/j.soilbio.2021.108153

Levia, D., Bischoff, S., Gruselle, M.-C., Näthe, K., Legates, D.R., Lutgen, A.N., Boyer, E.W., Michalzik, B., 2023. Geometric configurations of particulate matter in terrestrial solutions of a temperate beech forest. J. Aerosol Sci. 106196. https://doi.org/10.1016/J.JAEROSCI.2023.106196

Levia, D.F., Keim, R.F., Carlyle-Moses, D.E., Frost, E.E., 2011. Throughfall and Stemflow in Wooded Ecosystems, in: Forest Hydrology and Biogeochemistry. pp. 425–443. https://doi.org/10.1007/978-94-007-1363-5_21

Manirajan, B.A., Maisinger, C., Ratering, S., Rusch, V., Schwiertz, A., Cardinale, M., Schnell, S., 2018. Diversity, specificity, co-occurrence and hub taxa of the bacterial-fungal pollen microbiome. FEMS Microbiol. Ecol. 94, 112. https://doi.org/10.1093/femsec/fiy112

Martin, M., 2011. Cutadapt removes adapter sequences from high-throughput sequencing reads. EMBnet.journal 17, 10. https://doi.org/10.14806/ej.17.1.200

McMurdie, P.J., Holmes, S., 2013. Phyloseq: an R package for reproducible interactive

analysis and graphics of microbiome census data. PLoS One 8, e61217. https://doi.org/10.1371/journal.pone.0061217

Michalzik, B., Kalbitz, K., Park, J.H., Solinger, S., Matzner, E., 2001. Fluxes and concentrations of dissolved organic carbon and nitrogen - A synthesis for temperate forests. Biogeochemistry 52, 173–205. https://doi.org/10.1023/A:1006441620810

Mori, T., Wang, S., Zhang, W., Mo, J., 2019. A potential source of soil ecoenzymes: From the phyllosphere to soil via throughfall. Appl. Soil Ecol. 139, 25–28. https://doi.org/10.1016/j.apsoil.2019.02.004

Ogle, D., Wheeler, P., Dinno, A., 2020. FSA: Fisheries Stock Analysis. R package version 0.8.31.

Ponette-González, A.G., Van Stan, J.T., Magyar, D., 2020. Things seen and unseen in throughfall and stemflow, in: Precipitation Partitioning by Vegetation: A Global Synthesis. Springer, Cham, pp. 70–87. https://doi.org/10.1007/978-3-030-29702-2_5

Potthast, K., Meyer, S., Crecelius, A.C., Schubert, U.S., Tischer, A., Michalzik, B., 2017. Land-use and fire drive temporal patterns of soil solution chemistry and nutrient fluxes. Sci. Total Environ. 605–606, 514–526. https://doi.org/10.1016/J.SCITOTENV.2017.06.182

Quast, C., Pruesse, E., Yilmaz, P., Gerken, J., Schweer, T., Yarza, P., Peplies, J., Glöckner, F.O., 2013. The SILVA ribosomal RNA gene database project: improved data processing and web-based tools. Nucleic Acids Res. 41, 590–596. https://doi.org/10.1093/nar/gks1219

Reche, I., D'Orta, G., Mladenov, N., Winget, D.M., Suttle, C.A., 2018. Deposition rates of viruses and bacteria above the atmospheric boundary layer. ISME J. 12, 1154–1162. https://doi.org/10.1038/s41396-017-0042-4

Sadeghi, S.M.M., Gordon, D.A., Van Stan, J.T., 2020. A global synthesis of throughfall and stemflow hydrometeorology, in: Precipitation Partitioning by Vegetation: A Global Synthesis. Springer International Publishing, pp. 48–69. https://doi.org/10.1007/978-3-030-29702-2_4

Sánchez-Parra, B., Núñez, A., García, A.M., Campoy, P., Moreno, D.A., 2021. Distribution of airborne pollen, fungi and bacteria at four altitudes using high-throughput DNA sequencing. Atmos. Res. 249, 105306. https://doi.org/10.1016/j.atmosres.2020.105306

Scheiner, D., 1974. A modified version of the sodium salicylate method for analysis of wastewater nitrates. Water Res. 8, 835–840. https://doi.org/10.1016/0043-1354(74)90030-X

Seelmeyer, G., 1954. Deutsche Einheitsverfahren zur Wasseruntersuchung. Herausgegeben im Auftrage der Fachgruppe Wasserchemie in der Gesellschaft Deutscher Chemiker E. V. Bearbeitet von L. W. Haase, H. Stooff, G. Gad, W. Wesly u.a. Verlag Chemie, Weinheim/Bergstraße 1954, 180. Mater. Corros. 5, 357–357. https://doi.org/10.1002/maco.19540050819

Stoddard, S.F., Smith, B.J., Hein, R., Roller, B.R.K., Schmidt, T.M., 2015. rrnDB: Improved tools for interpreting rRNA gene abundance in bacteria and archaea and a new foundation for future development. Nucleic Acids Res. 43, 593–598. https://doi.org/10.1093/nar/gku1201

Takai, K., Horikoshi, K., 2000. Rapid detection and quantification of members of the archaeal community by quantitative PCR using fluorogenic probes. Appl. Environ. Microbiol. 66, 5066–5072. https://doi.org/10.1128/AEM.66.11.5066-5072.2000

Teachey, M.E., Pound, P., Ottesen, E.A., Van Stan, J.T., 2018. Bacterial community

composition of throughfall and stemflow. Front. For. Glob. Chang. 1. https://doi.org/10.3389/ffgc.2018.00007

Team, R.C., 2020. A Language and Environment for Statistical Computing. R Found. Stat. Comput.

Van Stan, J.T., Morris, C.E., Aung, K., Kuzyakov, Y., Magyar, D., Rebollar, E.A., Remus-Emsermann, M., Uroz, S., Vandenkoornhuyse, P., 2020. Precipitation partitioning—hydrologic highways between microbial communities of the plant microbiome?, in: Precipitation Partitioning by Vegetation: A Global Synthesis. Springer International Publishing, pp. 228–251. https://doi.org/10.1007/978-3-030-29702-2_14

Van Stan, J.T., Ponette-González, A.G., Swanson, T., Weathers, K.C., 2021. Throughfall and stemflow are major hydrologic highways for particulate traffic through tree canopies. Front. Ecol. Environ. 19, 404–410. https://doi.org/10.1002/fee.2360

Van Stan, J.T., Stubbins, A., 2018. Tree-DOM: Dissolved organic matter in throughfall and stemflow. Limnol. Oceanogr. Lett. 3, 199–214. https://doi.org/10.1002/lol2.10059

Van Stan, J.T., Wagner, S., Guillemette, F., Whitetree, A., Lewis, J., Silva, L., Stubbins, A., 2017. Temporal Dynamics in the Concentration, Flux, and Optical Properties of Tree-Derived Dissolved Organic Matter in an Epiphyte-Laden Oak-Cedar Forest. J. Geophys. Res. Biogeosciences 122, 2982–2997. https://doi.org/10.1002/2017JG004111

Vorholt, J.A., 2012. Microbial life in the phyllosphere. Nat. Rev. Microbiol. 10, 828-840. https://doi.org/10.1038/nrmicro2910

Vrede, K., Heldal, M., Norland, S., Bratbak, G., 2002. Elemental composition (C, N, P) and cell volume of exponentially growing and nutrient-limited bacterioplankton. Appl. Environ. Microbiol. 68, 2965–2971. https://doi.org/10.1128/AEM.68.6.2965-2971.2002

Figure Captions

Figure 1: Study site and study design for sample collection at the Hainich Critical Zone Exploratory in western Thuringia, Germany. A) Sampling was conducted at an open area-site for rainwater representative of above-canopy precipitation and at a mixed beech forest site for phyllosphere, throughfall, stemflow, and seepage and soil sampling at different depths. B) Number of samples for each compartment during one sampling event. Sampling took place in May and September 2020. Soil was only collected in May. C) Conceptional representation of samples spanning from the tree canopy down to the soil, and photographs of the two tree species, sample collectors and a typical soil core.

Figure 2: Bacterial transport across the different compartments, and contributions and correlations to transported carbon and nitrogen. **A)** Fluxes of TOC and TN expressed per m^2 h^{-1}, bacterial contributions to TOC and TN content, and fluxes of bacterial cells per m^2 h^{-1} across the different compartments during an early and late growing season rain event. Each symbol represents a single sample, and the crossbar depicts the average for each compartment. Significant differences are shown in letter code tested by post hoc Dunn's multiple comparing ($p < 0.05$). **B)** Spearman's rank correlation (r_s) between bacterial cell flux per m^2 h^{-1} and TOC and TN of water fluxes per m^2 h^{-1} in May and September.

Figure 3: Bacterial communities across rainwater (n = 8), leaves (n = 48), throughfall (n = 20), stemflow (n = 8), seepage (n = 25) and soil (n = 34) samples. **A)** Observed ASV richness (left panel) and Shannon index (right panel). Single data points are shown as dots for samples from May and triangles from September (crossbar represents mean of values). Letter code indicates significant differences between compartments and indexes after Dunn's post hoc test ($p < 0.05$). **B)** Distribution of most abundant bacterial families depicted as NMDS based on Bray-Curtis dissimilarities across all samples. Results of PERMANOVA (9999

789 permutations) are displayed as Venn diagram, asterisks depict confidence interval at $p < 0.001$
790 for each accounting factor. **C)** Bacterial community composition of most abundant bacterial
791 families with more than 1 % absolute read abundance per sampling point. Single stacked bars
792 show the relative read abundance of 16S rRNA gene sequences on family level.

793

794 **Figure 4:** Prediction of metabolic functions of bacterial communities across the different
795 compartments and the two time points. **A)** Abundance of KEGG orthologues (KO)
796 corresponding to genes for enzymes of selected metabolic pathways. The size of the bubbles
797 depicts the mean relative KO abundance of each compartment. **B)** Proportions of bacterial
798 communities employing the predicted KO. Small dots depict the mean relative abundance of
799 bacterial classes per sample and the bigger dots represent the mean relative abundance for
800 a given compartment. Letter code displays significant differences between compartments
801 within each pathway based on post hoc Dunn's multiple comparing ($p < 0.05$).

802

803 **Figure 5:** Phylogeny and relative abundance of bacterial core taxa across rainwater,
804 phyllosphere, throughfall, stemflow and seepage samples during both sampling time points.
805 The tree is based on a neighbor-joining model of a 16S rRNA gene alignment. The color and
806 shape of each node show the presence of an ASV on family-level and on genus-level,
807 respectively, at a given compartment. The size of nodes depicts the mean relative abundance
808 of each ASV across the compartments. Stacked bars display the mean relative abundance of
809 each ASV across all samples from both sampling points of rain, phyllosphere, throughfall,
810 stemflow and seepage communities.

811

812

813

Datasets

Dataset 1: microbial gene and cell abundance, carbon and nitrogen concentrations, cell and matter fluxes

Dataset 2: Relative abundance of most abundant bacterial families

Dataset 3: Estimated total abundance of bacterial families and contributions to TOC and TN

Dataset 4: Relative abundance of predicted KO IDs for metagenomic pathways and of bacterial communities employing predicted KO IDs based on PICRUSt2 analysis

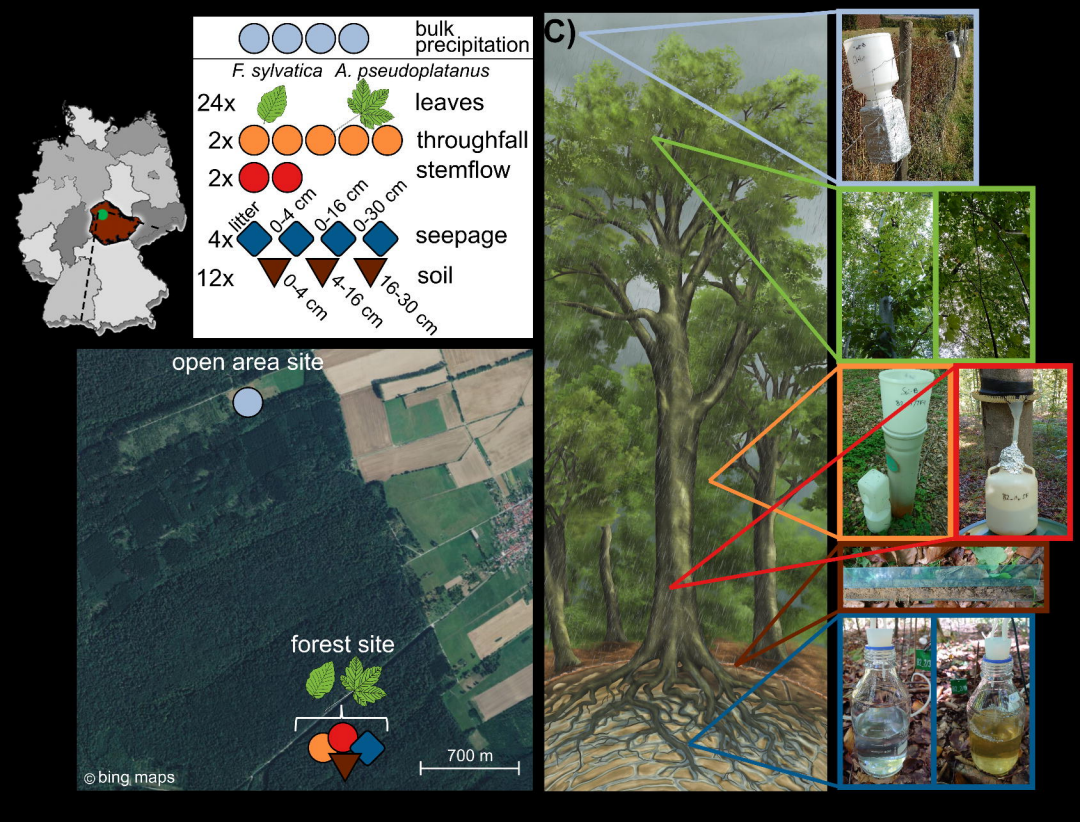
bulk precipitation
F. sylvatica
A. pseudoplatanus
24x
leaves
2x
throughfall
2x
stemflow
litter
0-4 cm
0-16 cm
0-30 cm
4x
seepage
12x
0-4 cm
4-16 cm
16-30 cm
soil
open area site
forest site
700 m
© bing maps
C)

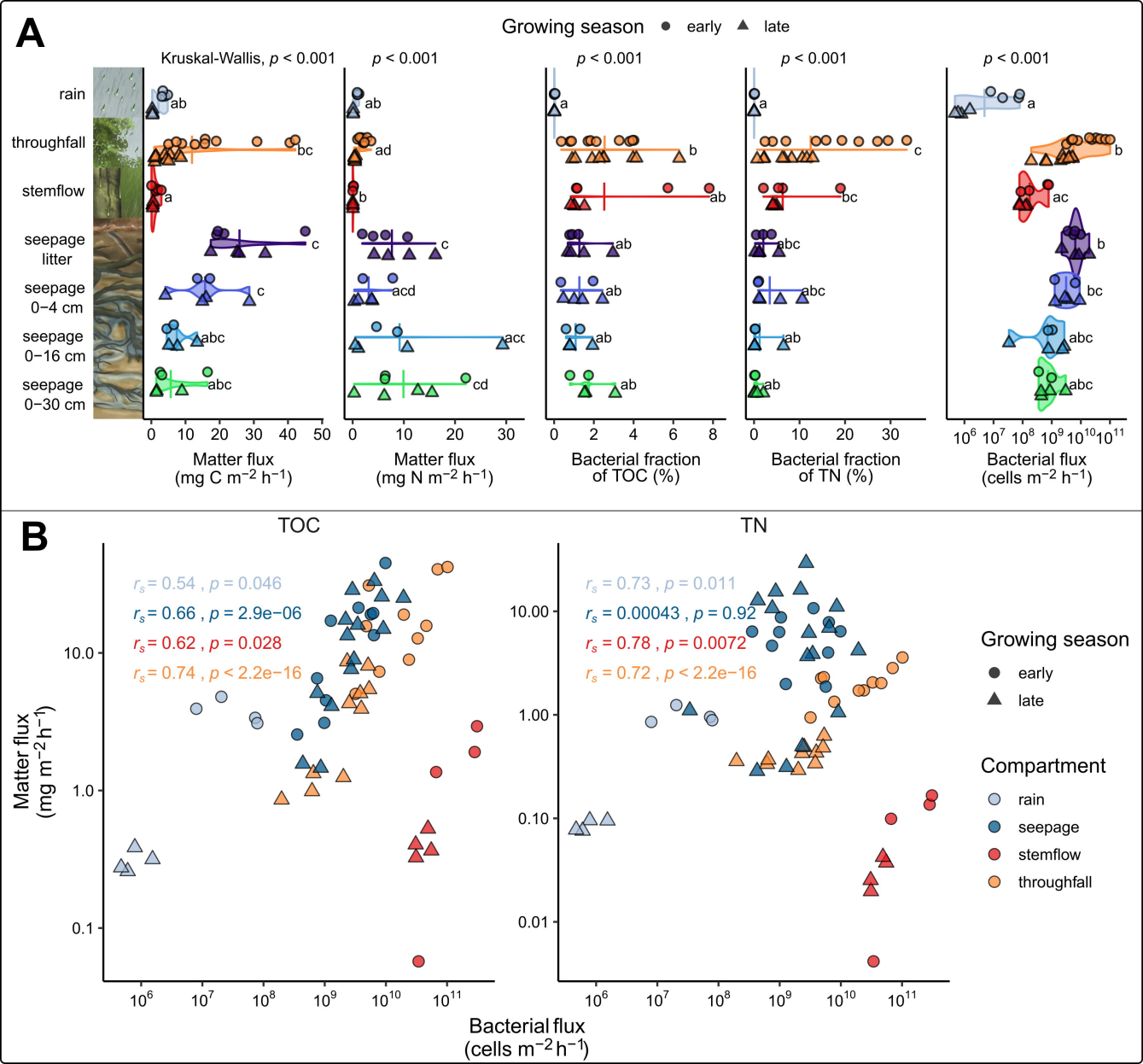
A
Growing season
early
late
Kruskal-Wallis, p < 0.001
p < 0.001
p < 0.001
p < 0.001
p < 0.001
rain
throughfall
stemflow
seepage litter
seepage 0–4 cm
seepage 0–16 cm
seepage 0–30 cm
Matter flux (mg C m−2 h−1)
Matter flux (mg N m−2 h−1)
Bacterial fraction of TOC (%)
Bacterial fraction of TN (%)
Bacterial flux (cells m−2 h−1)
B
TOC
TN
rs = 0.54 , p = 0.046
rs = 0.66 , p = 2.9e−06
rs = 0.62 , p = 0.028
rs = 0.74 , p < 2.2e−16
rs = 0.73 , p = 0.011
rs = 0.00043 , p = 0.92
rs = 0.78 , p = 0.0072
rs = 0.72 , p < 2.2e−16
Matter flux (mg m−2 h−1)
Bacterial flux (cells m−2 h−1)
Growing season
early
late
Compartment
rain
seepage
stemflow
throughfall

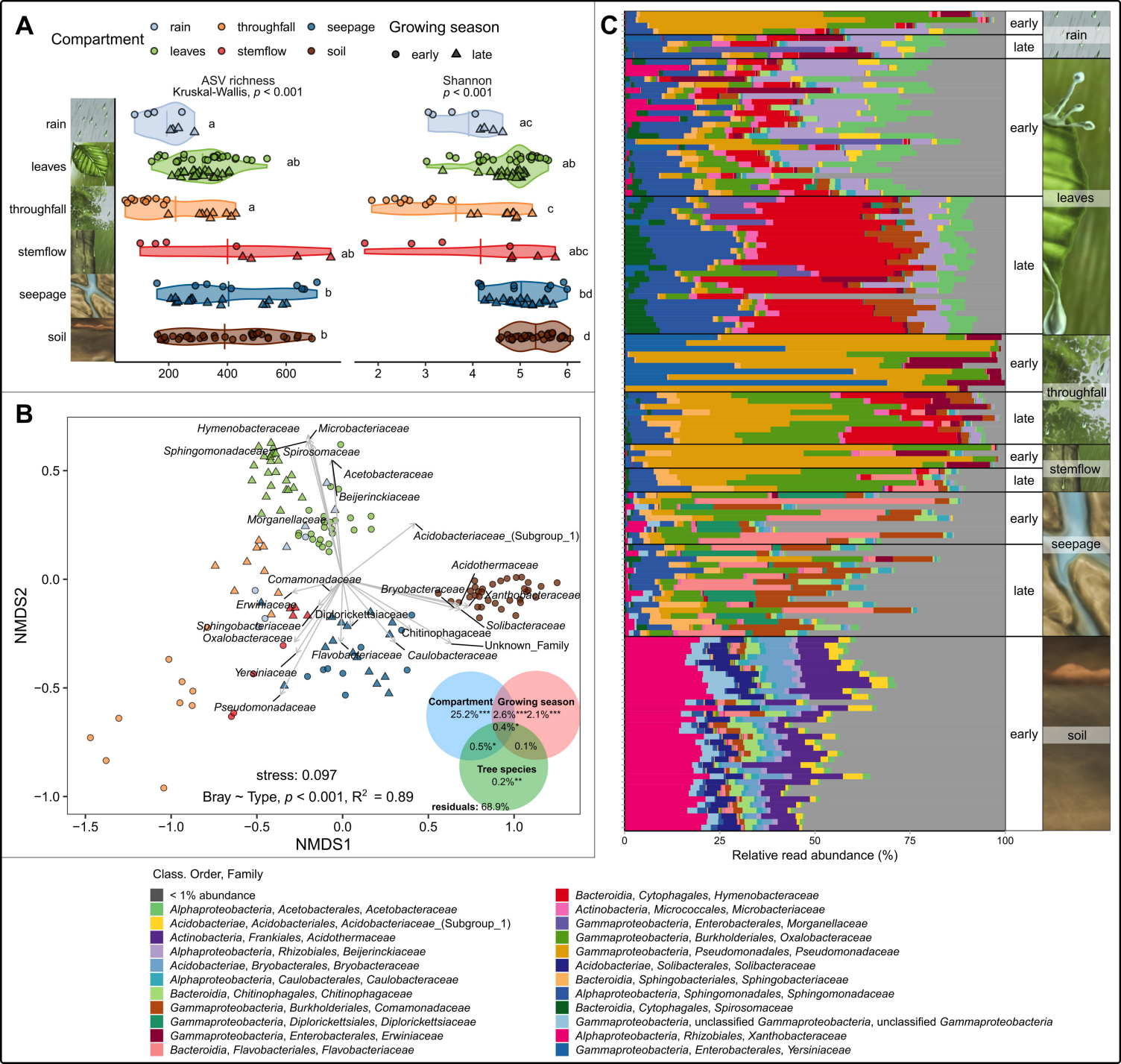
A
Compartment
rain
throughfall
seepage
leaves
stemflow
soil
Growing season
early
late
ASV richness
Kruskal-Wallis, p < 0.001
Shannon
p < 0.001
rain
leaves
throughfall
stemflow
seepage
soil
a
ab
a
ab
b
b
ac
ab
c
abc
bd
d
200
400
600
2
3
4
5
6
B
Hymenobacteraceae
Microbacteriaceae
Sphingomonadaceae
Spirosomaceae
Acetobacteraceae
Beijerinckiaceae
Morganellaceae
Acidobacteriaceae_(Subgroup_1)
Acidothermaceae
Comamonadaceae
Bryobacteraceae
Xanthobacteraceae
Erwiniaceae
Diplorickettsiaceae
Solibacteraceae
Sphingobacteriaceae
Oxalobacteraceae
Chitinophagaceae
Unknown_Family
Flavobacteriaceae
Caulobacteraceae
Yersiniaceae
Pseudomonadaceae
Compartment
25.2%***
Growing season
2.6%***
2.1%***
0.4%*
0.5%*
0.1%
Tree species
0.2%**
residuals: 68.9%
stress: 0.097
Bray ~ Type, p < 0.001, R2 = 0.89
NMDS2
NMDS1
0.5
0.0
−0.5
−1.0
−1.5
−1.0
−0.5
0.0
0.5
1.0
C
early
late
rain
leaves
throughfall
stemflow
seepage
soil
0
25
50
75
100
Relative read abundance (%)
Class. Order, Family
< 1% abundance
Alphaproteobacteria, Acetobacterales, Acetobacteraceae
Acidobacteriae, Acidobacteriales, Acidobacteriaceae_(Subgroup_1)
Actinobacteria, Frankiales, Acidothermaceae
Alphaproteobacteria, Rhizobiales, Beijerinckiaceae
Acidobacteriae, Bryobacterales, Bryobacteraceae
Alphaproteobacteria, Caulobacterales, Caulobacteraceae
Bacteroidia, Chitinophagales, Chitinophagaceae
Gammaproteobacteria, Burkholderiales, Comamonadaceae
Gammaproteobacteria, Diplorickettsiales, Diplorickettsiaceae
Gammaproteobacteria, Enterobacterales, Erwiniaceae
Bacteroidia, Flavobacteriales, Flavobacteriaceae
Bacteroidia, Cytophagales, Hymenobacteraceae
Actinobacteria, Micrococcales, Microbacteriaceae
Gammaproteobacteria, Enterobacterales, Morganellaceae
Gammaproteobacteria, Burkholderiales, Oxalobacteraceae
Gammaproteobacteria, Pseudomonadales, Pseudomonadaceae
Acidobacteriae, Solibacterales, Solibacteraceae
Bacteroidia, Sphingobacteriales, Sphingobacteriaceae
Alphaproteobacteria, Sphingomonadales, Sphingomonadaceae
Bacteroidia, Cytophagales, Spirosomaceae
Gammaproteobacteria, unclassified Gammaproteobacteria, unclassified Gammaproteobacteria
Alphaproteobacteria, Rhizobiales, Xanthobacteraceae
Gammaproteobacteria, Enterobacterales, Yersiniaceae

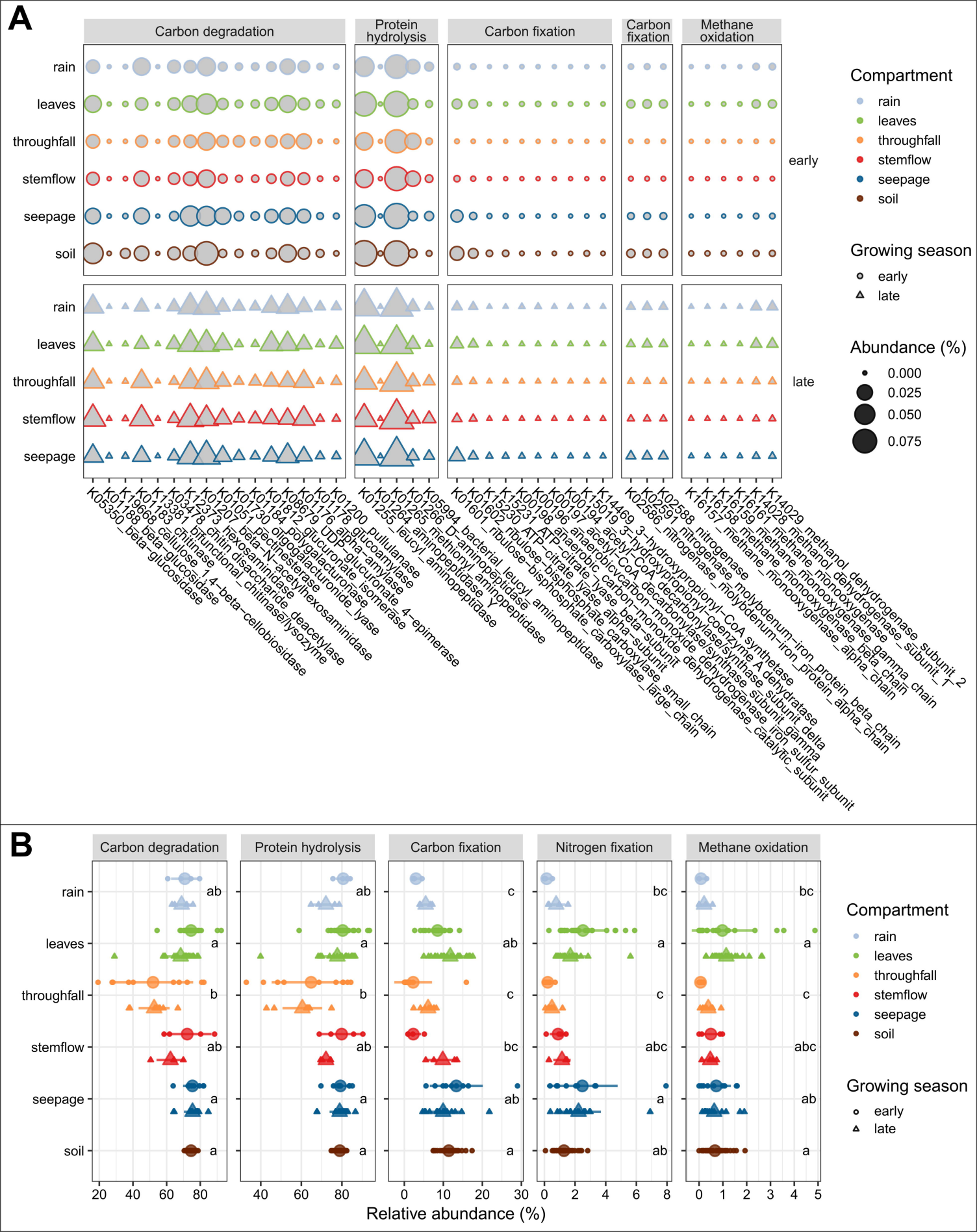
A
Carbon degradation
Protein hydrolysis
Carbon fixation
Carbon fixation
Methane oxidation
rain
leaves
throughfall
stemflow
seepage
soil
early
late
Compartment
rain
leaves
throughfall
stemflow
seepage
soil
Growing season
early
late
Abundance (%)
0.000
0.025
0.050
0.075
K05350_beta-glucosidase
K01188_beta-glucosidase
K19668_cellulose_1,4-beta-cellobiosidase
K01183_chitinase
K13381_chitin_disaccharide_deacetylase
K03478_bifunctional_chitinase/lysozyme
K12373_hexosaminidase
K01207_beta-N-acetylhexosaminidase
K01051_pectinesterase
K01730_oligogalacturonide_lyase
K01184_polygalacturonase
K01812_glucuronate_isomerase
K08679_UDP-glucuronate_4-epimerase
K01176_alpha-amylase
K01178_glucoamylase
K01200_pullulanase
K01255_leucyl_aminopeptidase
K01264_aminopeptidase Y
K01265_methionyl_aminopeptidase
K01266_D-aminopeptidase
K05994_bacterial_leucyl_aminopeptidase
K01601_ribulose-bisphosphate_carboxylase_large_chain
K01602_ribulose-bisphosphate_carboxylase_small_chain
K15230_ATP-citrate_lyase_alpha-subunit
K15231_ATP-citrate_lyase_beta-subunit
K00198_anaerobicvcarbon-monoxide dehydrogenase_catalytic_subunit
K00196_anaerobicvcarbon-monoxide dehydrogenase_iron sulfur subunit
K00197_acetyl-CoA decarbonylase/synthase subunit_gamma
K00194_acetyl-CoA decarbonylase/synthase subunit_delta
K15019_acetyl-CoA synthetase
K14469_3-hydroxypropionyl-coenzyme A dehydratase
K02586_nitrogenase_molybdenum-iron_protein_alpha_chain
K02591_nitrogenase_molybdenum-iron_protein_beta_chain
K02588_nitrogenase_molybdenum-iron_protein_gamma_chain
K16157_methane_monooxygenase_alpha_chain
K16158_methane_monooxygenase_beta_chain
K16159_methane_monooxygenase_gamma_chain
K16161_methane_monooxygenase_subunit_T_2
K14028_methanol_dehydrogenase_subunit_1
K14029_methanol_dehydrogenase_subunit_2
B
Carbon degradation
Protein hydrolysis
Carbon fixation
Nitrogen fixation
Methane oxidation
rain
leaves
throughfall
stemflow
seepage
soil
ab
a
b
ab
a
a
c
ab
c
bc
ab
a
bc
a
c
abc
a
ab
bc
a
c
abc
ab
a
20
40
60
80
40
60
80
0
10
20
30
0
2
4
6
8
0
1
2
3
4
5
Relative abundance (%)
Compartment
rain
leaves
throughfall
stemflow
seepage
soil
Growing season
early
late

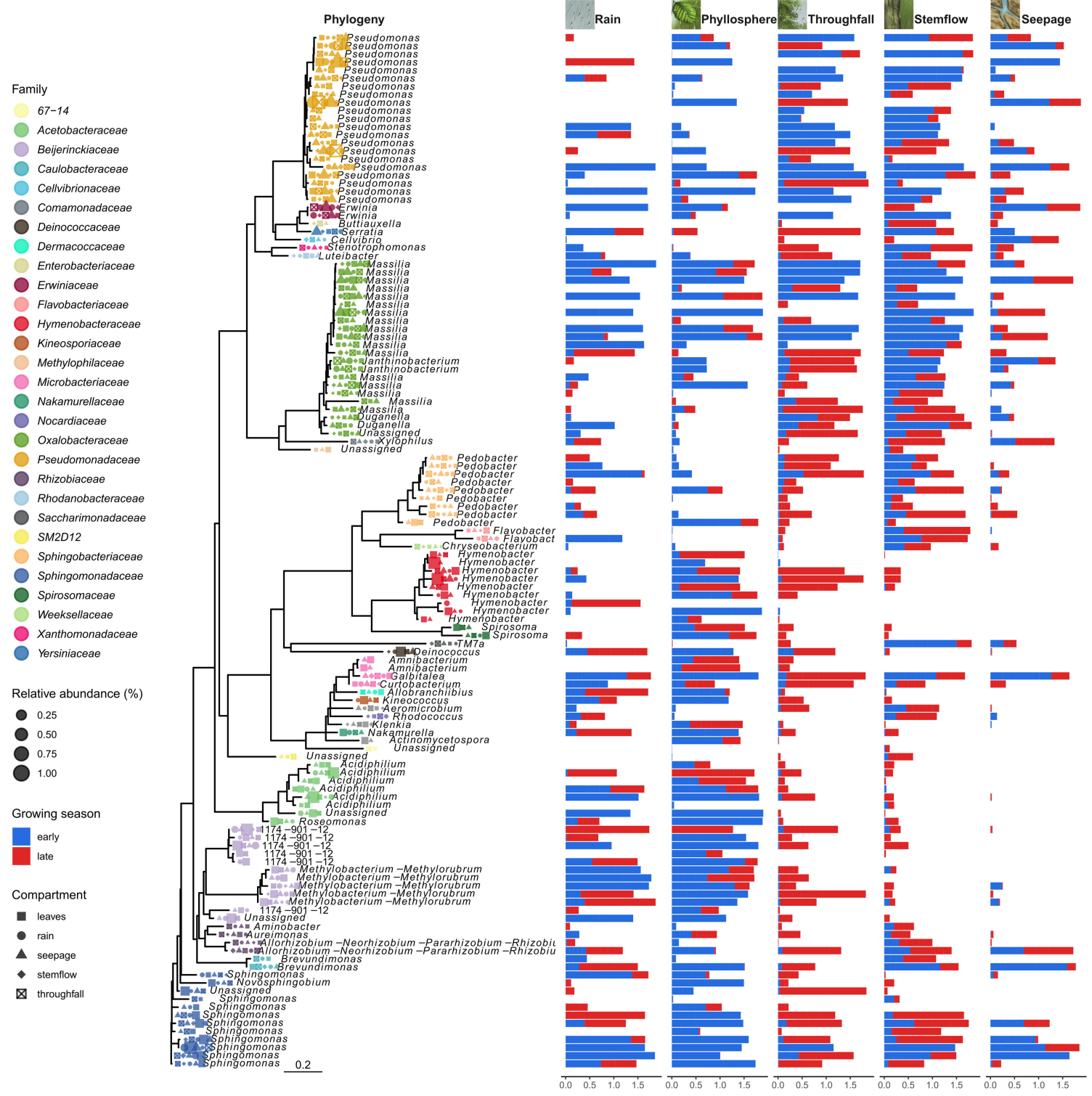
Phylogeny
Rain
Phyllosphere
Throughfall
Stemflow
Seepage
Family
67−14
Acetobacteraceae
Beijerinckiaceae
Caulobacteraceae
Cellvibrionaceae
Comamonadaceae
Deinococcaceae
Dermacoccaceae
Enterobacteriaceae
Erwiniaceae
Flavobacteriaceae
Hymenobacteraceae
Kineosporiaceae
Methylophilaceae
Microbacteriaceae
Nakamurellaceae
Nocardiaceae
Oxalobacteraceae
Pseudomonadaceae
Rhizobiaceae
Rhodanobacteraceae
Saccharimonadaceae
SM2D12
Sphingobacteriaceae
Sphingomonadaceae
Spirosomaceae
Weeksellaceae
Xanthomonadaceae
Yersiniaceae
Relative abundance (%)
0.25
0.50
0.75
1.00
Growing season
early
late
Compartment
leaves
rain
seepage
stemflow
throughfall
Pseudomonas
Erwinia
Buttiauxella
Serratia
Cellvibrio
Stenotrophomonas
Luteibacter
Massilia
Xanthinobacterium
Duganella
Unassigned
Xylophilus
Pedobacter
Flavobacter
Chryseobacterium
Hymenobacter
Spirosoma
TM7a
Deinococcus
Amnibacterium
Galbitalea
Curtobacterium
Allobranchiibius
Kineococcus
Aeromicrobium
Rhodococcus
Klenkia
Nakamurella
Actinomycetospora
Acidiphilium
Roseomonas
1174 −901 −12
Methylobacterium −Methylorubrum
Aminobacter
Aureimonas
Allorhizobium −Neorhizobium −Pararhizobium −Rhizobiu
Brevundimonas
Sphingomonas
Novosphingobium
0.2
0.0
0.5
1.0
1.5